Billion-Fold Increase in Tip-Enhanced Raman Signal

H. Kumar Wickramasinghe,[†,*] Marc Chaigneau,[‡] Ryohei Yasukuni,[‡] Gennaro Picardi,[‡] and Razvigor Ossikovski[‡,*]

[†]Department of Electrical Engineering and Computer Science, University of California, Irvine, California 92697, United States and [‡]LPICM, Ecole Polytechnique, CNRS, 91128 Palaiseau, France

ABSTRACT A billion-fold increase in the Raman signal over conventional tip-enhanced Raman spectroscopy/microscopy (TERS) is reported. It is achieved by introducing a stimulating beam confocal with the pump beam into a conventional TERS setup. A stimulated TERS spectrum, closely corresponding to its spontaneous TERS counterpart, is obtained by plotting the signal intensity of the strongest Raman peak of an azobenzene thiol self-assembled monolayer *versus* the stimulating laser frequency. The stimulated TERS image of azobenzene thiol molecules grafted onto Au ⟨111⟩ clearly shows the surface distribution of the molecules, whereas, when compared to the simultaneously recorded surface topography, it presents an image contrast of different nature. The experimentally obtained stimulated gain is estimated at 1.0×10^9, which is in reasonable agreement with the theoretically predicted value. In addition to the signal increase, the signal-to-noise ratio was 3 orders of magnitude higher than in conventional spontaneous TERS. The proposed stimulated TERS technique offers the possibility for a substantially faster imaging of the surface with respect to normal TERS.

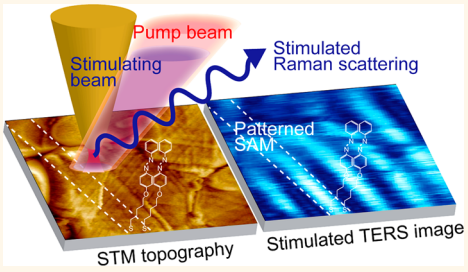

KEYWORDS: tip-enhanced Raman spectroscopy · stimulated Raman · surface chemical imaging · self-assembled monolayer

Tip-enhanced Raman spectroscopy (TERS) combines Raman spectroscopy with scanning probe microscopy (SPM).[1−5] The increase of the Raman signal is due to a strong electromagnetic (EM) field enhancement at the SPM tip apex related to localized surface plasmon resonance (LSPR) excitation. This results in the generation of sufficient photon counts to record Raman signals with adequate signal-to-noise (S/N) ratios at reasonable time frames. Since the original proposal of Wessel,[1] and the initial demonstrations of TERS,[2−5] the past decade has seen extraordinary development in TERS activity.[6−10] The main properties of TERS are its high spatial resolution and its high sensitivity. Comparison of SPM topographic and Raman chemical images provides unique surface information, making TERS a valuable technique for surface analysis. Today, TERS applications are expanding not only in the field of physical chemistry but also in biology.[11−13] However, typical spectral acquisition times with adequate S/N ratios are more than a few hundred milliseconds, which limits applications, especially for imaging. The TERS field can benefit substantially from any technique, for instance, based on a nonlinear Raman effect,[14,15] that can enhance the S/N ratio, thus allowing for a reduced acquisition time.

Stimulated emission is a well-known phenomenon that boosts molecular emission rate.[16] It has been applied successfully to stimulated Raman scattering (SRS) microscopy[17,18] and femtosecond stimulated Raman spectroscopy (FSRS).[19−21] The sensitivity and S/N improvements have enabled real-time imaging of biological activity (for SRS) and the femtosecond-scale tracking of conformational changes within molecules (for FSRS). Since conventional TERS is based on spontaneous Raman emission, a stimulated emission process could also improve the sensitivity and the S/N ratio of TERS.

In this paper, we demonstrate that both the signal and the S/N ratio in TERS can be significantly enhanced by using the stimulated emission mechanism. A collinear, tunable stimulating beam was introduced along with a polarization-modulated pump beam into a conventional TERS setup. The stimulated signal was measured by lock-in detection. Initial results on stimulated TERS

* Address correspondence to (H. K. Wickramasinghe) hkwick@uci.edu or (R. Ossikovski) razvigor.ossikovski@polytechnique.edu.

Received for review December 6, 2013 and accepted March 6, 2014.

Published online March 06, 2014
10.1021/nn406263m

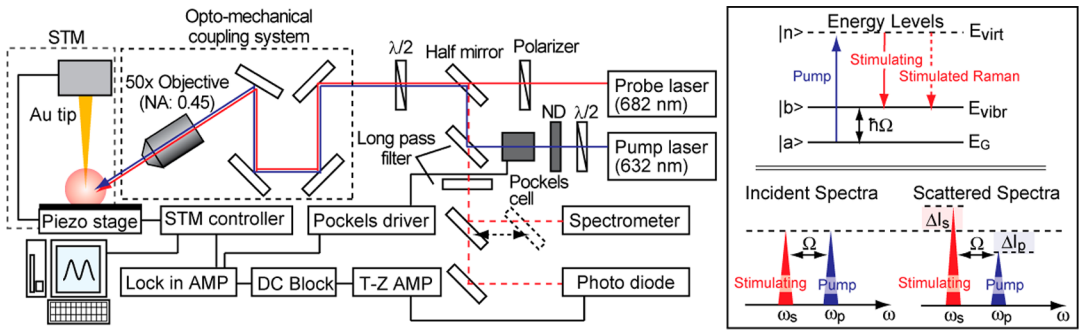

Figure 1. Schematic of the stimulated TERS (sTERS) experiment.

images of a [4-(phenylazo)phenoxy]hexane-1-thiol (azobenzene thiol) self-assembled monolayer (SAM) grafted onto a Au ⟨111⟩ surface are presented and compared with the simultaneously recorded surface topography. We also discuss the stimulated signal gain and S/N ratio in comparison to conventional TERS.

RESULTS AND DISCUSSION

Referring to Figure 1, in a conventional TERS experiment, the tip is illuminated only by the pump beam. The pump field, which excites the molecule to a virtual state $|n\rangle$, interacts with the zero-point field to generate a coherence between the ground state $|a\rangle$ and the vibrational state $|b\rangle$. The pump field and the zero-point field scatter off this $a-b$ coherence to promote the molecule to the excited vibrational state $|b\rangle$ while emitting a Stokes photon. The $a \rightarrow b$ transition rate and Stokes intensity are proportional to the pump field intensity. The stimulated TERS (sTERS) situation is similar except that the zero-point field is replaced by an intense stimulating field. In this situation, pump and stimulating photon pairs create an $a-b$ coherence, and the next pump−probe photon pair scatters off this coherence to promote the molecule to the excited vibrational state $|b\rangle$ while emitting a Stokes photon. The $a \rightarrow b$ transition rate in this case is proportional to the product of the pump laser intensity and the stimulating laser intensity and therefore can be orders of magnitude higher.[22] The ratio of the stimulated Raman cross section to the spontaneous Raman cross section (the stimulated gain G) is given by

$$G = \sigma_{STIM}/\sigma_{SPON} = [32\pi^3 c^2/\omega_s^2]F(\omega_s) \qquad (1)$$

where $F(\omega_s)$ is the spectral photon flux of the stimulating beam in photons/s/m^2/Hz.[23]

By taking a 0.7 mW stimulating power at λ_{Stokes} = 682 nm and a laser bandwidth = 64 GHz (our experimental condition) and assuming a representative electromagnetic field enhancement of 100 in the gap between a gold surface and a gold tip (value derived from estimations from our experiment (see Supporting Information), as well as from numerical calculations in TERS[24,25]) we theoretically get $G = 3.3 \times 10^9$ for the stimulated gain from eq 1. This means that the stimulated Stokes signal can be 3.3×10^9 times the spontaneous TERS signal and could easily be detected without the need for photon counters.

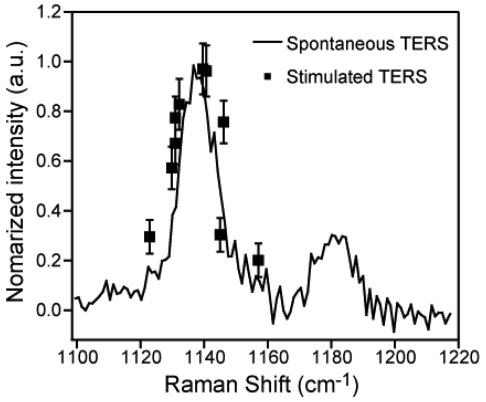

Figure 2. sTERS spectrum of the 1142 cm^{-1} vibration mode of azobenzene recorded over a SAM of azobenzene thiol on gold. The error bar shows standard deviation of the lock-in signal fluctuations. STM parameters: current set point I = 0.05 nA, bias voltage V = −0.5 V; sTERS parameters: pump power P_P = 0.5 mW, stimulating beam power P_S = 0.5 mW, lock-in time constant T = 100 ms, load resistance R_L = 100 kΩ.

The schematic of our sTERS experiment is shown in Figure 1. Stimulated Raman experiments normally require lock-in detection to detect small intensity changes of pump or stimulating beam. Pulsed lasers are generally used for modulating the pump or the stimulating beam intensity, together with lock-in detection.[18] We achieved the modulation with a continuous wave laser by varying the pump beam polarization using a Pockels cell. With a P polarized pump beam (electric field oscillating along with the tip axis), gap mode surface plasmon resonances are more efficiently excited between the gold surface and the tip.[24,25] Thus, pump laser power was modulated between P and S polarizations to alternate between the TERS condition (electromagnetic enhancement operating) and unenhanced scattering. The plasmon resonances also contribute to increase the photon flux of the stimulating beam under the tip.

Figure 2 shows a sTERS spectrum obtained by plotting the lock-in signal amplitude as a function of the stimulating beam wavelength. The emission wavelength

of the stimulating laser was tuned from 681.2 nm to 682.8 nm (corresponding to a Raman shift from 1123 cm^{-1} to 1158 cm^{-1}, with respect to 632.8 nm excitation) through the 1142 cm^{-1} azobenzene thiol peak (in-phase stretching of the two phenyl−N bonds of the azobenzene moiety)[26] by regulating the temperature of the laser diode. The laser intensity was maintained at about 0.5 mW at each emission wavelength. A flat homogeneous area on the fully azobenzene covered gold surface was selected prior to experiments with the STM. The probed position was changed between measurements in order to avoid the decrease in the Raman signal due to photobleaching of the molecules. The full-width at half-maximum value of the stimulating beam was between 2 and 4 cm^{-1}.

The sTERS spectrum compares well with the spontaneous TERS spectrum of azobenzene thiol on gold recorded with the same setup, indicating that the detected lock-in signal is neither due to spontaneous Raman nor just a scattered/reflected pump beam.

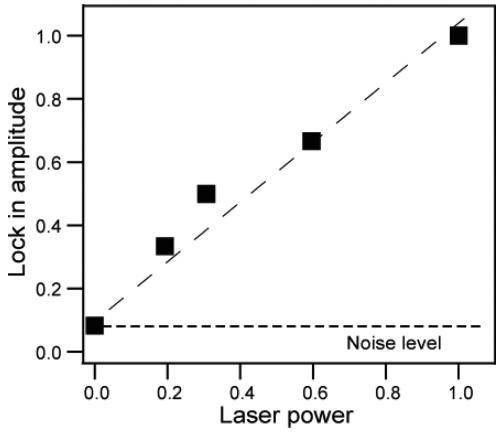

Figure 3. Lock-in signal amplitudes plotted as functions of the stimulating beam intensities. Both *x* and *y* axes are normalized. The dashed line is a linear guide for the eye. STM parameters: I_S = 0.05 nA, V = −0.5 V; sTERS parameters: P_P = 0.5 mW, P_S = 0.2 to 1 mW, T = 100 ms, R_L = 1 MΩ.

Since the spectral resolution in sTERS is primarily determined by the line widths of the pump laser and the stimulating tunable laser rather than the resolution of the grating spectrometer used in conventional spontaneous TERS, the use of narrow bandwidth tunable lasers enables a substantial improvement in the achievable spectral resolution.

Lock in signal amplitudes were also plotted as a function of the stimulating beam intensities in Figure 3. The stimulating beam intensity was varied from 0.2 to 1.0 mW by using neutral density (ND) filters. Lock-in amplitude is linearly proportional to the stimulating laser intensity, as predicted by eq 1.

Figure 4a,b display the simultaneously recorded STM image and sTERS image of a patterned azobenzene SAM formed by nanocontact printing. The original stamp has a grating structure with a 300 nm width and a 300 nm pitch. Triangular features attesting to the ⟨111⟩ surface reconstruction can be recognized in Figure 4a. The azobenzene SAM pattern, whose thickness is expected to be about 2 nm,[27,28] is not distinguished in our STM image at room temperature under ambient conditions, possibly due to the presence of ambient contamination and limited *z* resolution. Conversely, the sTERS image contrast clearly shows the grating structure of the contact printing stamp, proving that we specifically detected the azobenzene distribution on the gold surface.

The sTERS image was recorded simultaneously with the STM topography in 14 min. The spatial resolution of a sTERS image in the *x* (fast scan) axis is experimentally limited to the product of the scan rate (here, 0.3 Hz), scan range (2000 nm), and lock-in time constant (0.1 s) adopted. In the *y* (slow scan) axis, the resolution is limited by the scan range divided by the number of lines per image, as in STM topography (256). To record a conventional TERS map over the same 2 × 2 μm^2 area with the same number of pixels (33 × 256) would take more than 2 h (assuming 1 s acquisition time for each pixel of the TERS mapping).

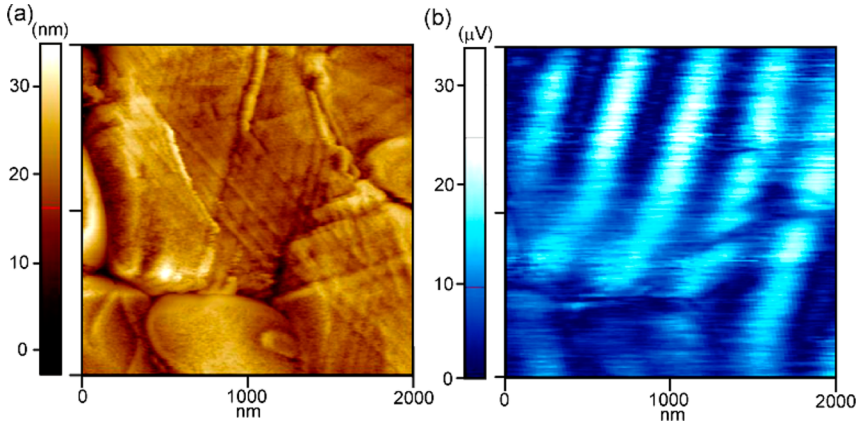

Figure 4. Set of (a) STM and (b) sTERS scans of patterned azobenzene thiol on Au ⟨111⟩. The scan area is 2000 nm × 2000 nm. STM parameters: current set point I_S = 0.05 nA, bias voltage V = −0.5 V; sTERS parameters: pump power P_P = 0.5 mW, stimulating beam power P_S = 1 mW, lock-in time constant T = 100 ms, scan rate R = 0.3 Hz, load resistor R_L = 1 MΩ.

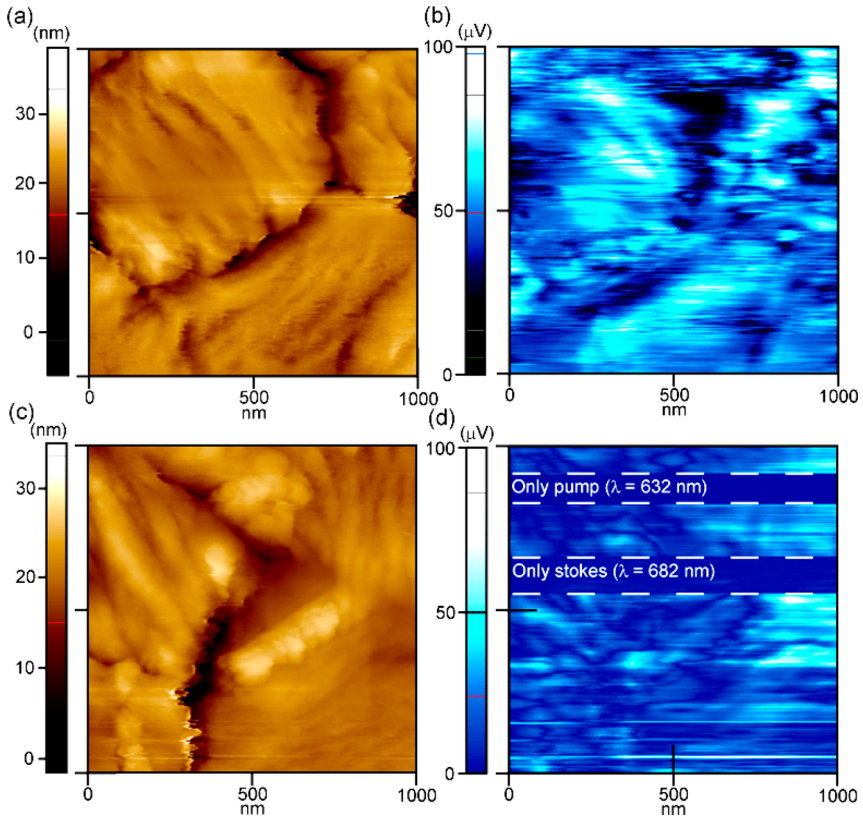

Figure 5. (a, b) Set of STM and sTERS scans of azobenzene thiol grafted on Au ⟨111⟩ by dip coating. STM parameters: current set point I_S = 0.05 nA, bias voltage V = −0.5 V; sTERS parameters: pump power P_P = 0.25 mW, stimulating beam power P_S = 0.7 mW, lock-in time constant T = 100 ms, scan rate R = 0.3 Hz, load resistor R_L = 100 kΩ. (c, d) Set of STM and sTERS scans with pump or stimulating beam momentarily blocked. STM parameters: I_S = 0.05 nA, V = −0.5 V; sTERS parameters: P_P = 0.5 mW, P_S = 1 mW, T = 100 ms, scan rate R = 0.3 Hz, R_L = 100 kΩ. Scan field = 1000 nm × 1000 nm.

Figure 5a,b show STM and corresponding sTERS images of a gold surface exposed to the azobenzene thiol solution in ethanol. The sTERS image is not uniform, although thiol molecules are expected to cover the entire surface. Moreover, the contrast in the sTERS image does not fully correspond to that of the STM image. To confirm that we indeed have stimulated Raman contrast and to compare the signal and noise levels of the stimulated TERS signal with respect to the spontaneous TERS, we momentarily blocked the stimulating and pump beams in succession while recording an image (shown in Figure 5c,d). The stimulating beam was blocked in the area noted as "only pump", whereas the pump beam was kept on, corresponding to spontaneous TERS conditions. In the area noted as "only stimulating", the pump beam was blocked and the stimulating beam was maintained. Both the pump and the stimulating beams were active in the rest of the image. In either case, the lock-in amplitude went down to almost zero. From the results above, it can be unambiguously inferred that we detected a stimulated Raman signal.

Variations in the gap field enhancement due to the uneven surface topography of the gold surface may contribute to the contrast observed in Figure 5b.[29] Additionally, finer contrast may be related to the probed molecular system. Molecular domains having the terminal azobenzene groups oriented exactly parallel to the tip−sample gap axis will most efficiently couple with the enhanced field. Minor variations in the molecular tilt angle will result in only subnanometric changes of the molecular layer thickness,[30] not resolved in the large-area STM topographic images but observable as contrast in the sTERS Raman images. We believe that variations in molecular orientations can therefore be one possible explanation for the contrast differences between the STM and sTERS images.

Figure 6a,b are STM and sTERS images of a smaller scan area. Again, contrast differences are observed between the sTERS image and the STM image. Figure 6c is a zoom of a small-molecular domain in the sTERS image from Figure 6b, showing a feature of 6 nm width, thus indicating that a spatial resolution of less than 6 nm is achieved (see the line scan across the feature in Figure 6d). This spatial resolution is better than what is achieved with conventional TERS imaging performed on the same setup.[31] Stimulated emission effectively occurred in the gap mode plasmon localized in a small junction between the tip and gold surface, resulting in a high spatial resolution.

Finally, we estimate the measured stimulated TERS gain and S/N ratio in comparison to conventional TERS.

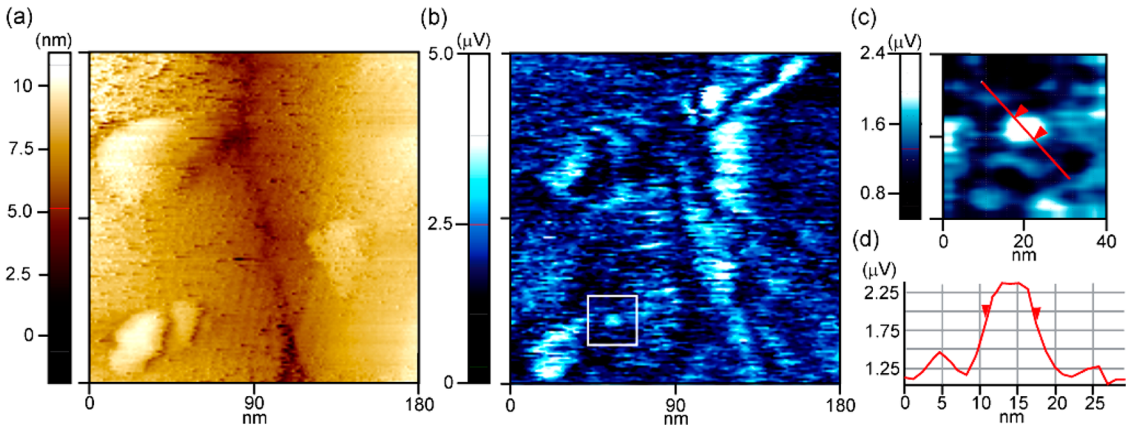

Figure 6. Comparison of (a) STM and (b) sTERS images of azobenzene thiol grafted on Au ⟨111⟩ with smaller scan field (180 nm × 180 nm). (c) Zoom of a feature contained in the white square in the sTERS image from (b). (d) Line scan across the feature from (c). STM parameters: current set point I_S = 0.05 nA, bias voltage V = −0.05 V; sTERS parameters: pump power P_P = 0.5 mW, stimulating beam power P_S = 0.5 mW, lock-in time constant T = 100 ms, scan rate R = 0.2 Hz, load resistor R_L = 100 kΩ.

We first calibrated the linearity of the lock-in for the detection of the small optical modulations by using the Pockels cell to amplitude modulate the HeNe laser and focusing the latter onto the same photodiode/lock-in detection setup as before. For a 100 kΩ load resistor and a lock-in signal of 100 μV at 100 ms time constant as used in our experiments (Figure 5b), the detected power was estimated to be 30 nW from the calibration (supplementary Figure S1). The mean value of the spontaneous TERS signal from azobenzene measured with the spectrometer under the same pump laser power is 100 photons/s, corresponding to 3×10^{-8} nW and an S/N of 10 in 1 Hz bandwidth. Thus, the stimulated gain G is estimated as 30 nW/3×10^{-8} nW, or 1.0×10^9, reasonably close to our theoretical estimation; see the Supporting Information. The S/N ratio of the sTERS signal is 2×10^3 in 1 Hz bandwidth. Although we are limited by electronic noise rather than by shot noise in the present setup, we note that for truly shot noise limited operation the S/N = $i_{signal}/(2e\Delta f)$ (i_{signal}: signal current, e: the electric charge, Δf: bandwidth), and the achievable S/N ratio would be 3.1×10^9 for our 100 μV signal and 100 kΩ load resistor in a 1 Hz bandwidth.

CONCLUSION

We demonstrated stimulated emission in tip-enhanced Raman spectroscopy. The wide-area (>1 μm^2) STM topography and sTERS images were recorded simultaneously with a very high spatial resolution at a scan rate of 0.2 to 0.3 Hz. While the current setup is not shot noise limited, shot noise limiting the detection scheme will enable a substantial increase in the achievable S/N at reasonable stimulating power. It is noteworthy that the present imaging rate is limited not by signal acquisition time but rather by the STM scanning rate to avoid tip damaging. Thanks to the achieved billion-fold stimulated gain over conventional TERS, our technique opens venues for ultrafast imaging applications in the TERS field.

METHODS

Materials. STM: Park Systems XE-100; Pockels cell: DIDA concept, EO/1M-400-N; photodiode: Thorlabs, DET10A; grating spectrometer: HORIBA Jobin Yvon, LabRAM HR 800; optomechanical XYZ translation system: HORIBA Jobin Yvon; tunable diode laser: Thorlabs, TCLDM9; transimpedance amplifier: Femto Messtechnik GmbH, DLPCA-200; lock-in amplifier: EG&G Princeton Applied Research, model 5210; STM tip: electrochemically etched 250 μm diameter gold wire (Goodfellow) with tip apex 20 nm; gold substrate: Arrandee 12 mm × 12 mm; nanocontact printing stamp: High-Tech Optics Ltd.

Sample Preparation. In all experiments, 250 nm Au films on a 2.5 nm Cr adhesion layer deposited on glass slides were used; these were flame annealed to promote ⟨111⟩ gold faceting. Synthesis of the [4-(phenylazo)phenoxy]hexane-1-thiol (azobenzene thiol) molecules is described elsewhere.[26] A self-assembled monolayer of azobenzene thiol was formed by immersing the Au ⟨111⟩ substrate in 1 mM azobenzene thiol ethanol solution. The nanocontact printing technique was used to obtain patterned SAMs using a poly(dimethylsiloxane) stamp with grating structure (width and interval of 300 nm).[32] A drop of 1 mM azobenzene thiol ethanol solution was deposited on the stamp. After drying, the nanograting was rinsed with ethanol to remove the excess molecules and dried by nitrogen flow. The grating pattern was transferred onto the Au ⟨111⟩ surface by gently pressing for 10 s.

Stimulated TERS Setup. Electrochemically etched gold wire tips with apex radii of around 20 nm were used as STM probes. The STM parameters are indicated in the figure captions. A pump He−Ne laser (632.8 nm) is transmitted through a Pockels cell polarization modulator, reflected off a high-pass dichroic filter (cut-off wavelength a few nanometers above 632.8 nm), and combined at a half-silvered mirror with a stimulating (Stokes), single mode, fiber-coupled tunable diode laser. Variable neutral density filters were used to control the laser power. The nominal pump laser power was 0.5 mW. The diode Stokes laser was tuned to 682.06 nm to stimulate the 1142 cm^{-1} azobenzene normal vibrational mode during image acquisition. A $\lambda/2$ plate in front of the Stokes beam provides P polarization of light. The combined beams are directed to a 0.45 NA, 50× Olympus objective (housed within an optomechanical XYZ translation

system and oriented at 60° with respect to the sample normal) and focused on the tip apex. Inserted in the pump path, the Pockels cell is sinusoidally driven at 30 kHz and orientated so that its output polarization is modulated between P and S at the STM tip. The backscattered light returns *via* the half-silvered mirror to a silicon photodiode after two long-pass filters (see dashed line in Figure 1). Alternatively, the backscattered light can be directed to a high-resolution grating spectrometer for recording a spontaneous TERS spectrum. The modulated photodiode current is converted to a voltage in a transimpedance amplifier and detected with a lock-in. The controller records the lock-in signal and displays a sTERS image simultaneously with an STM image as the sample is raster scanned.

Conflict of Interest: The authors declare no competing financial interest.

Acknowledgment. H.K.W. is grateful to Prof, Ossikovski at Ecole Polytechnique for hosting his sabbatical stay in Paris. He would also like to acknowledge the support of NSF CaSTL subaward 2007-06015-02. Two of the authors (R.O. and M.C.) gratefully recognize financial support from the General Directorate for Research (DGAR) of Ecole Polytechnique as well as from the Thematic Network for Advanced Research (RTRA) "Triangle de la Physique". M.C. is grateful to the R&D Raman Division of HORIBA Jobin Yvon for technical support. The authors are indebted to V. Popov from High-Tech Optics Ltd. for having provided them with the nanograting stamp.

Supporting Information Available: Description of the theoretical calculation of stimulated Raman gain and the calibration of lock-in signal amplitudes. This material is available free of charge *via* the Internet at http://pubs.acs.org.

REFERENCES AND NOTES

1. Wessel, J. Surface-Enhanced Optical Microscopy. *J. Opt. Soc. Am. B* **1985**, *2*, 1538–1541.
2. Stockle, R. M.; Suh, Y. D.; Deckert, V.; Zenobi, R. Nanoscale Chemical Analysis by Tip-Enhanced Raman Spectroscopy. *Chem. Phys. Lett.* **2000**, *318*, 131–136.
3. Anderson, M. S. Locally Enhanced Raman Spectroscopy with an Atomic Force Microscope. *Appl. Phys. Lett.* **2000**, *76*, 3130–3132.
4. Hayazawa, N.; Inouye, Y.; Sekkat, Z.; Kawata, S. Metallized Tip Amplification of Near-Field Raman Scattering. *Opt. Commun.* **2000**, *183*, 333–336.
5. Pettinger, B.; Picardi, G.; Schuster, R.; Ertl, G. Surface Enhanced Raman Spectroscopy: Towards Single Molecular Spectroscopy. *Electrochemistry (Tokyo, Jpn.)* **2000**, *68*, 942–949.
6. Schmid, T.; Yeo, B. S.; Leong, G.; Stadler, J.; Zenobi, R. Performing Tip-Enhanced Raman Spectroscopy in Liquids. *J. Raman Spectrosc.* **2009**, *40*, 1392–1399.
7. Stadler, J.; Schmid, T.; Zenobi, R. Nanoscale Chemical Imaging Using Top-Illuminated Tip-Enhanced Raman Spectroscopy. *Nano Lett.* **2010**, *10*, 4514–4520.
8. Pettinger, B.; Schambach, P.; Villagomez, C. J.; Scott, N. Tip-Enhanced Raman Spectroscopy: Near-Fields Acting on a Few Molecules. *Annu. Rev. Phys. Chem.* **2012**, *63*, 379–399.
9. Schmid, T.; Opilik, L.; Blum, C.; Zenobi, R. Nanoscale Chemical Imaging Using Tip Enhanced Raman Spectroscopy. *Angew. Chem., Int. Ed.* **2013**, *52*, 5940–5945.
10. Yu, J.; Saito, Y.; Ichimura, T.; Kawata, S.; Verma, P. Far-Field Free Tapping-Mode Tip-Enahnced Raman Microscopy. *Appl. Phys. Lett.* **2013**, *102*, 123110.
11. Pozzi, E. A.; Sonntag, M. D.; Jiang, N.; Klingsporn, J. M.; Hersam, M. C.; Van Duyne, R. P. Tip Enhanced Raman Imaging: An Emergent Tool for Probing Biology at the Nanoscale. *ACS Nano* **2013**, *7*, 885–888.
12. Kuroski, D.; Deckert-Gaudig, T.; Deckert, V.; Lednev, I. K. Structure and Composition of Insulin Fibril Surfaces Probed by TERS. *J. Am. Chem. Soc.* **2012**, *134*, 13323–13329.
13. Blum, C.; Schmid, T.; Opilik, L.; Weidmann, S.; Fagerer, S. R.; Zenobi, R. Understanding Tip-Enhanced Raman Spectra of Biological Molecules: A Combined Raman, SERS and TERS Study. *J. Raman Spectrosc.* **2012**, *43*, 1895–1904.
14. Ichimura, T.; Hayazawa, N.; Hashimoto, M.; Inouye, Y.; Kawata, S. Tip-Enhanced Coherent Anti-Stokes Raman Scattering for Vibrational Nanoimaging. *Phys. Rev. Lett.* **2004**, *92*, 220801.
15. Zhang, R.; Zhang, Y.; Dong, Z. C.; Jiang, S.; Zhang, C.; Chen, L. G.; Zhang, L.; Liao, Y.; Aizpurua, J.; Luo, Y.; Yang, J. L.; Hou, J. G. Chemical Mapping of a Single Molecule by Plasmon-Enhanced Raman Scattering. *Nature* **2013**, *498*, 82–86.
16. Einstein, A. On the Quantum Theory of Radiation. *Phys. Z.* **1917**, *18*, 121.
17. Freudiger, C. W.; Min, W.; Saar, B. G.; Lu, S.; Holtom, G. R.; He, C.; Tsai, J. C.; Kang, J. X.; Xie, X. S. Label-Free Biomedical Imaging with High Sensitivity by Stimulated Raman Scattering Microscopy. *Science* **2008**, *322*, 1857–1860.
18. Ozeki, Y.; Kitagawa, Y.; Sumimura, K.; Nishizawa, N.; Umemura, W.; Kajiyama, S.; Itho, K. Stimulated Raman Scattering Microscope with Shot Noise Limited Sensitivity Using Subharmonically Synchronized Laser Pulses. *Opt. Express.* **2010**, *18*, 13708–13719.
19. Kukura, P.; McCamant, D. W.; Mathies, R. A. Femtosecond Stimulated Raman Spectroscopy. *Annu. Rev. Phys. Chem.* **2007**, *58*, 461–488.
20. Frontiera, R. R.; Henry, A. I.; Gruenke, N. L.; Van Duyne, R. P. Surface-Enahnced Femtosecond Stimulated Raman Spectroscopy. *J. Phys. Chem. Lett.* **2011**, *2*, 1199–1203.
21. Lanin, A. A.; Fedotov, I. V.; Fedotov, A. B.; Sidorov-Biryukov, D. A.; Zheltikov, A. M. The Phase-Controlled Raman Effect. *Sci. Rep.* **2013**, *3*, 1842.
22. Potma, E. O.; Mukamel, S. In *Coherent Raman Scattering Microscopy*; Cheng, J. X., Xie, X. S., Eds.; CRC Press/Taylor & Francis Group, 2013; pp 4−35.
23. McCamant, D. W.; Kukura, P.; Mathies, R. A. Femtosecond Broadband Stimulated Raman: a New Approach for High-Performance Vibrational Spectroscopy. *Appl. Spectrosc.* **2003**, *57*, 1317–1323.
24. Downes, A.; Salter, D.; Elfick, A. Finite Element Simulations of Tip-Enhanced Raman and Fluorescence Spectroscopy. *J. Phys. Chem. B* **2006**, *110*, 6692–6698.
25. Yang, Z.; Aizpurua, J.; Xu, H. Electromagnetic Field Enhancement in TERS Configurations. *J. Raman Spectrosc.* **2009**, *40*, 1343–1348.
26. Picardi, G.; Chaigneau, M.; Ossikovski, R.; Licitra, C.; Delapierre, G. Tip Enhanced Raman Spectroscopyon Azobenzene Thiol Self-assembled Monolayers on Au(111). *J. Raman Spectrosc.* **2009**, *40*, 1407–1412.
27. Wolf, H.; Ringsdolf, H.; Delamarche, E.; Takami, T.; Kang, H.; Michel, B.; Gerber, Ch.; Jaschke, M.; Butt, H.-J.; Bamberg, E. End-Group-Dominated Molecular Order in Self-Assembled Monolayers. *J. Phys. Chem.* **1995**, *99*, 7102–7107.
28. Evans, S. D.; Johnson, S. R.; Ringsdorf, H.; Williams, L. M.; Wolf, H. Photoswitching of Azobenzene Derivatives Formed on Planar and Colloidal Gold Surfaces. *Langmuir* **1998**, *14*, 6436–6440.
29. Zhang, W.; Cui, X.; Yeo, B. S.; Schmid, T.; Hafner, C.; Zenobi, R. Nanoscale Roughness on Metal Surface Can Increase Tip-Enhanced Raman Scattering by an Order of Magnitude. *Nano Lett.* **2007**, *7*, 1401–1405.
30. Mannsfeld, S. C. B.; Canzler, T. W.; Fritz, T.; Proehl, H.; Leo, K.; Stumpf, S.; Goretzki, G.; Gloe, K. The Structure of [4-(Phenylazo)phenoxy]hexane-1-thiol Self-Assembled Monolayers on Au(111). *J. Phys. Chem. B* **2002**, *106*, 2255–2260.
31. Picardi, G.; Chaigneau, M.; Ossikovski, R. High Resolution Probing of Multi Wall Carbon Nanotubes by Tip Enhanced Raman Spectroscopy in Gap-Mode. *Chem. Phys. Lett.* **2009**, *469*, 161–165.
32. Stadler, J.; Schmid, T.; Opilik, L.; Kuhn, P.; Dittrich, P. S.; Zenobi, R. Tip-Enhanced Raman Spectroscopy Imaging of Patterned Thiol Monolayers. *Beilstein J. Nanotechnol.* **2011**, *2*, 509–515.